

EXISTENCE AND LOCAL UNIQUENESS FOR 3D SELF-CONSISTENT MULTISCALE MODELS OF FIELD-EFFECT SENSORS*

STEFAN BAUMGARTNER[†] AND CLEMENS HEITZINGER[‡]

Abstract. We present existence and local uniqueness theorems for a system of partial differential equations modeling field-effect nano-sensors. The system consists of the Poisson(-Boltzmann) equation and the drift-diffusion equations coupled with a homogenized boundary layer. The existence proof is based on the Leray-Schauder fixed-point theorem and a maximum principle is used to obtain a-priori estimates for the electric potential, the electron density, and the hole density. Local uniqueness around the equilibrium state is obtained from the implicit-function theorem. Due to the multiscale problem inherent in field-effect biosensors, a homogenized equation for the potential with interface conditions at a surface is used. These interface conditions depend on the surface-charge density and the dipole-moment density in the boundary layer and still admit existence and local uniqueness of the solution when certain conditions are satisfied. Due to the geometry and the boundary conditions of the physical system, the three-dimensional case must be considered in simulations. Therefore a finite-volume discretization of the 3d self-consistent model was implemented to allow comparison of simulation and measurement. Special considerations regarding the implementation of the interface conditions are discussed so that there is no computational penalty when compared to the problem without interface conditions. Numerical simulation results are presented and very good quantitative agreement with current-voltage characteristics from experimental data of biosensors is found.

Key words. Existence, local uniqueness, system of elliptic PDEs, self-consistent model, homogenization, interface conditions, nanowire, field-effect sensor, biosensor, DNA sensor, gas sensor.

AMS subject classifications. 35A01, 35A02, 35J25, 35Q70, 65N06, 82D80.

1. Introduction

The objective of this work is to prove existence and local uniqueness of the solution of a system of partial differential equations that models field-effect sensors such as BioFETs (biologically sensitive field-effect transistors) and gas sensors in a self-consistent manner.

Field-effect biosensors have been realized in experiments using silicon nanowires in recent years [1–5]. Field-effect gas sensors [6–8] based on tin-oxide nanowires have been demonstrated as well. The basic working principle of BioFETs (see Figure 1.1) is that the binding of analyte molecules in a liquid to receptor molecules bound at the sensor surface changes the charge concentration at this surface. This affects the electrostatic potential in the semiconducting nanowire and the resulting conductance change is measured. The main advantage of these biosensors compared to current technology is label-free operation, i.e., no fluorescent or radioactive markers are needed. Furthermore, they provide high sensitivity, real-time operation, and high selectivity. The range of applications includes biomedicine, biotechnology, food and drug industries, environmental monitoring, and process technology.

*Received: April 22, 2011; accepted (in revised version): August 28, 2011. Communicated by Pierre Degond.

[†]Department of Mathematics and Wolfgang Pauli Institute, University of Vienna, A–1090 Vienna, Austria (Stefan.Baumgartner@univie.ac.at).

[‡]Department of Applied Mathematics and Theoretical Physics, University of Cambridge, Cambridge CB3 0WA, UK, and Department of Mathematics, University of Vienna, A–1090 Vienna, Austria (C.Heitzinger@damtp.cam.ac.uk).

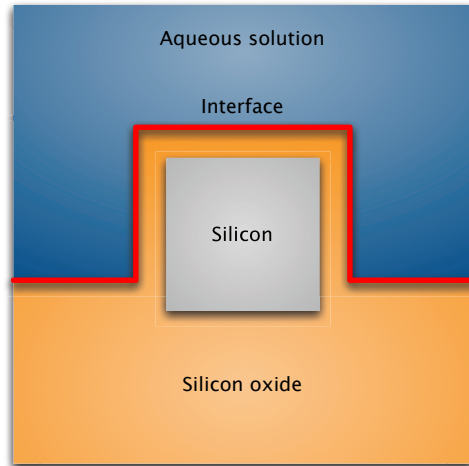


FIG. 1.1. *Schematic cross section through the biosensor. The boundary conditions are Dirichlet boundary conditions at the top, at the bottom, and at the contacts of the nanowire (not shown) and zero Neumann boundary conditions everywhere else.*

In the case of gas sensors, reducing or oxidizing gases react with the surface of the nanowire in reactions that are not fully understood. These reactions result in charge transfer from or to the nanowire surface. Again, this change in charge concentration of the nanowire modulates the current through the semiconducting nanowire. Applications include the detection of toxic gases such as CO and H₂S.

Despite the experimental progress, the detection mechanisms are not completely understood quantitatively and PDE models are important in order to gain insight into the physics and the behavior of such sensing devices and to help in their rational design.

Therefore a self-consistent model that accounts for the various free charge carriers is essential for field-effect sensors. The model discussed here is based on earlier work [9,10] and the geometry is based on experimental structures [2,11]. The simulation domain consists of three subdomains with different physical properties and hence different model equations. The first subdomain Ω_{Si} consists of the (silicon) nanowire and acts as the transducer of the sensor; in this subdomain, the drift-diffusion equations are used to model charge transport. The semiconductor is coated with a dielectric layer which comprises the second subdomain Ω_{ox} where the Poisson equation holds. In the third domain Ω_{liq} — the aqueous solution containing cations and anions — the Poisson-Boltzmann equation holds. Due to the geometry and the boundary conditions used in experiments, three-dimensional simulations are necessary.

The boundary layer at the sensor surface is responsible for recognition of the analyte molecules and requires special attention. In the case of biosensors, solving a homogenization problem gives rise to two interface conditions for the Poisson equation. These interface conditions depend on the surface-charge density and the dipole-moment density of the boundary layer [10,12]. In the case of gas sensors, the model for the surface charge is a system of ODEs that models surface reactions [13]. Both of these surface models are included in the following and consequently the results hold for both bio- and gas sensors.

This paper is organized as follows. In Section 2, the model equations are described in detail and the main result is stated. In Section 3, the existence of solutions of semi-linear elliptic problems with interface conditions is shown. Based on these lemmata, the existence of solutions of the model equations is proved in Section 4. Furthermore, in Section 5, we show local uniqueness of the solution around the equilibrium state, i.e., when the applied voltages are small enough. A discretization that retains the band structure of the problem without interface conditions is given in Section 6 so that numerical solutions can be calculated as fast as for the problem without interface conditions. Numerical results are shown in Section 7 and compared to experimental data. Finally Section 8 concludes the paper.

2. The model equations and statement of the main result

In this section, the self-consistent model is presented and the main result is stated. The domain $\Omega \subset \mathbb{R}^3$ is partitioned into three subdomains Ω_{Si} (silicon), Ω_{ox} (oxide), and Ω_{liq} (liquid), and an interface Γ between Ω_{ox} and Ω_{liq} (see Figure 1.1).

2.1. Homogenization and interface conditions. The fast varying spatial structure of the charge concentration in the boundary layer between the aqueous solution and the dielectric layer (shown red in Figure 1.1) gives rise to a multiscale problem which has been solved by a homogenization method [10]. This interface Γ splits the domain $\Omega \subset \mathbb{R}^3$ into two parts Ω^+ and Ω^- . For the sake of notational simplicity, we assume that the normal vector of the interface Γ points in the positive x -direction and is located at $x = 0$; the coordinates parallel to the interface are denoted by y . The idea is to replace the fast varying charge concentration by interface conditions that depend only on the slow variable.

Before homogenization, the boundary-value problem is

$$\begin{aligned} -\nabla \cdot (A \nabla V_\varepsilon) &= \rho_\varepsilon && \text{in } \Omega, \\ V_\varepsilon(0+, y) &= V_\varepsilon(0-, y) && \text{on } \Gamma, \\ A(0+) \partial_x V_\varepsilon(0+, y) &= A(0-) \partial_x V_\varepsilon(0-, y) && \text{on } \Gamma, \end{aligned}$$

where ρ_ε is a charge concentration that varies fast in Ω^+ near Γ , V_ε is the electrostatic potential, and A is the permittivity. The jump in the permittivity A gives rise to two continuity conditions: the continuity of the potential (the second equation of the system) and the continuity of the electric displacement field (the third equation).

The idea of the homogenization procedure is to compare the weak formulations of two problems: the first problem is the original problem above and the second, the homogenized problem, contains general interface conditions, but not the fast varying charge concentration. At the end of the procedure, the interface conditions are found by comparing the coefficients of the test function and its normal derivative with respect to the interface; since it is a second order problem, there are two interface conditions.

In summary, after homogenization, i.e., after $\varepsilon \rightarrow 0+$, the original boundary-value problem above becomes the homogenized boundary-value problem [10]

$$-\nabla \cdot (A \nabla V) = 0 \quad \text{in } \Omega^+, \tag{2.1a}$$

$$-\nabla \cdot (A \nabla V) = \rho \quad \text{in } \Omega^-, \tag{2.1b}$$

$$V(0+, y) - V(0-, y) = \alpha(y) \quad \text{on } \Gamma, \tag{2.1c}$$

$$A(0+) \partial_x V(0+, y) - A(0-) \partial_x V(0-, y) = \gamma(y) \quad \text{on } \Gamma. \tag{2.1d}$$

Here α is the macroscopic dipole-moment density and γ is the macroscopic surface-charge density of the boundary layer. The values of α and γ contain the cumulative effect of the fast varying charge concentration ρ_ε , but depend only on the slow variable.

A rigorous calculation of the microscopic charge interactions in the boundary layer has been realized by a Monte-Carlo algorithm in [14], from which the values of α and γ are obtained immediately.

2.2. The charge-transport model. The model is self-consistent; more precisely, the system of equations has the structure

$$\begin{aligned} V &= V(n, p, \alpha, \gamma), \\ n &= n(V, p), \\ p &= p(V, n), \\ \alpha &= M_\alpha(V), \\ \gamma &= M_\gamma(V), \end{aligned}$$

where n and p are the electron and hole concentrations in Ω_{Si} , respectively. In Ω_{Si} , V , n , and p are the solutions of the drift-diffusion equations [15–18]. The values α and γ of the interface conditions are given by microscopic models M_α and M_γ for the surface-charge density and dipole-moment density of the boundary layer. They generally depend on the electrostatic potential and usually on the electrostatic potential close to the boundary layer. The microscopic models M_α and M_γ have been realized, e.g., by Monte-Carlo simulations [14], by Poisson-Boltzmann calculations [19], or by systems of ordinary differential equations for surface reactions [13].

The latter case is relevant for gas sensors and the surface charge is computed from the solutions of systems of ODEs that govern the chemical reactions. These systems of ODEs have bounded C^1 solutions global in time. In the case of SnO_2 based sensors in the presence of oxygen and a reducing gas such as CO, the chemisorption and ionization at the surface can be described by the system

$$\begin{aligned} \frac{dN_O}{dt} &= k_1([S] - N_O - N_S)[O_2]^{1/2} - k_{-1}N_O - \frac{dN_S}{dt}, \\ \frac{dN_S}{dt} &= k_2n_sN_O - k_{-2}N_S, \end{aligned}$$

where N_O denotes the neutral-adsorbed-oxygen density, N_S is the ionized-oxygen density, and the k_i are the rate constants of the surface processes, while $[S]$ is the local adsorption-site density and $[O_2]$ is the oxygen concentration [13]. Furthermore the electron concentration n_s corresponds to the surface-charge density $M_\gamma(V)$, and the dipole moment density $M_\alpha(V)$ vanishes in the case of gas sensors since the distance from the surface is zero. Of course, there are many more systems of ODEs that are relevant for the modeling of gas sensors.

The charge transport in the semiconducting nanowire can be calculated by special models for confined structures [20–22]. In this work, the charge-transport equations in Ω_{Si} that yield the carrier concentrations n and p are the drift-diffusion-Poisson system

$$-\nabla \cdot (A \nabla V) = q(p - n + C_{\text{dop}}), \quad (2.2a)$$

$$\nabla \cdot J_n = R, \quad (2.2b)$$

$$\nabla \cdot J_p = -R, \quad (2.2c)$$

$$J_n = D_n \nabla n - \mu_n n \nabla V, \quad (2.2d)$$

$$J_p = -D_p \nabla p - \mu_p p \nabla V, \quad (2.2e)$$

where q is the elementary charge, C_{dop} is the doping concentration of the semiconductor, D_n and D_p are the diffusion coefficients of the charge carriers, μ_n and μ_p are their carrier mobilities, J_n and J_p are the current densities, and R is the recombination rate. The Shockley-Read-Hall recombination rate is defined as

$$R := \frac{np - n_i^2}{\tau_p(n + n_i) + \tau_n(p + n_i)}, \quad (2.3)$$

where n_i is the intrinsic charge density and τ_n and τ_p are the lifetimes of the free carriers. Furthermore we assume that the Einstein relations $D_n = U_T \mu_n$ and $D_p = U_T \mu_p$ hold, where U_T is the thermal voltage. In the Slotboom variables u and v , which are defined by

$$\begin{aligned} n &=: n_i e^{V/U_T} u, \\ p &=: n_i e^{-V/U_T} v, \end{aligned}$$

the system (2.2) becomes

$$\begin{aligned} -\nabla \cdot (A \nabla V) &= q n_i (e^{-V/U_T} v - e^{V/U_T} u) + q C_{\text{dop}}, \\ U_T n_i \nabla \cdot (\mu_n e^{V/U_T} \nabla u) &= n_i \frac{uv - 1}{\tau_p (e^{V/U_T} u + 1) + \tau_n (e^{-V/U_T} v + 1)}, \\ U_T n_i \nabla \cdot (\mu_p e^{-V/U_T} \nabla v) &= n_i \frac{uv - 1}{\tau_p (e^{V/U_T} u + 1) + \tau_n (e^{-V/U_T} v + 1)}. \end{aligned}$$

The boundary is partitioned into Dirichlet and Neumann boundaries. The Dirichlet conditions

$$V|_{\partial\Omega_D} = V_D, \quad u|_{\partial\Omega_{\text{Si},D}} = u_D, \quad v|_{\partial\Omega_{\text{Si},D}} = v_D$$

hold at the ohmic contacts $\partial\Omega_{\text{Si},D}$, which are located at the source and drain contacts of the semiconductor. For details about the boundary conditions at the ohmic contacts the reader is referred to [16]. A voltage across the simulation domain in the vertical direction can be applied as well, i.e., an electrode in the liquid and a back-gate contact at the bottom of the structure are also part of $\partial\Omega_D$. The zero Neumann conditions

$$\nabla_\nu V|_{\partial\Omega_N} = 0, \quad \nabla_\nu u|_{\partial\Omega_{\text{Si},N}} = 0, \quad \nabla_\nu v|_{\partial\Omega_{\text{Si},N}} = 0$$

hold on the Neumann part $\partial\Omega_N$ of the boundary.

2.3. The liquid. The equation for the aqueous solution Ω_{liq} is the Poisson-Boltzmann model

$$-\nabla \cdot (A \nabla V) = \sum_{\sigma} \sigma \eta e^{-\sigma \beta (V - \Phi)},$$

where η is the ionic concentration, the constant β is defined as $\beta := q/(kT)$ in terms of the Boltzmann constant k and the temperature T , and Φ is the Fermi level. The right-hand side is a sum over the valences σ of all ion species; for example, the index set $\sigma \in \{-1, +1\}$ corresponds to a 1:1 electrolyte such as Na^+Cl^- . In this case, the equation simplifies to

$$-\nabla \cdot (A \nabla V) = -2\eta \sinh(\beta(V - \Phi)).$$

2.4. The model equations. In summary, the model is the boundary-value problem

$$-\nabla \cdot (A \nabla V) = qC_{\text{dop}} - qn_i(e^{V/U_T}u - e^{-V/U_T}v) \quad \text{in } \Omega_{\text{Si}}, \tag{2.4a}$$

$$-\nabla \cdot (A \nabla V) = 0 \quad \text{in } \Omega_{\text{ox}}, \tag{2.4b}$$

$$-\nabla \cdot (A \nabla V) = -2\eta \sinh(\beta(V - \Phi)) \quad \text{in } \Omega_{\text{liq}}, \tag{2.4c}$$

$$V(0+, y) - V(0-, y) = \alpha \quad \text{on } \Gamma, \tag{2.4d}$$

$$A(0+)\partial_x V(0+, y) - A(0-)\partial_x V(0-, y) = \gamma \quad \text{on } \Gamma, \tag{2.4e}$$

$$U_T n_i \nabla \cdot (\mu_n e^{V/U_T} \nabla u) = n_i \frac{uv-1}{\tau_p(e^{V/U_T}u+1) + \tau_n(e^{-V/U_T}v+1)} \quad \text{in } \Omega_{\text{Si}}, \tag{2.4f}$$

$$U_T n_i \nabla \cdot (\mu_p e^{-V/U_T} \nabla v) = n_i \frac{uv-1}{\tau_p(e^{V/U_T}u+1) + \tau_n(e^{-V/U_T}v+1)} \quad \text{in } \Omega_{\text{Si}}, \tag{2.4g}$$

$$\alpha = M_\alpha(V) \quad \text{on } \Gamma, \tag{2.4h}$$

$$\gamma = M_\gamma(V) \quad \text{on } \Gamma, \tag{2.4i}$$

$$V = V_D \quad \text{on } \partial\Omega_D, \tag{2.4j}$$

$$u = u_D, \quad v = v_D \quad \text{on } \partial\Omega_{D,\text{Si}}, \tag{2.4k}$$

$$\nabla_\nu V = 0 \quad \text{on } \partial\Omega_N, \tag{2.4l}$$

$$\nabla_\nu u = 0, \quad \nabla_\nu v = 0 \quad \text{on } \partial\Omega_{N,\text{Si}}. \tag{2.4m}$$

2.5. Statement of the main result. In order to state the main result, the coefficients and boundary conditions in the boundary-value problem (2.4) have to satisfy the following assumptions.

ASSUMPTIONS 2.1.

- (i) *The bounded domain $\Omega \subset \mathbb{R}^3$ has a C^2 Dirichlet boundary $\partial\Omega_D$, the Neumann boundary $\partial\Omega_N$ consists of C^2 segments, and the Lebesgue measure of the Dirichlet boundary $\partial\Omega_D$ is nonzero. The C^2 hypersurface $\Gamma \subset \Omega$ splits the domain Ω into two nonempty domains Ω^+ and Ω^- so that $\text{meas}(\Gamma \cap \partial\Omega) = 0$ and $\Gamma \cap \partial\Omega \subset \partial\Omega_N$ hold.*
- (ii) *The coefficient functions A , μ_n , and μ_p are uniformly elliptic and bounded with $A|_{\Omega^+} \in C^1(\Omega^+, \mathbb{R}^{3 \times 3})$, $A|_{\Omega^-} \in C^1(\Omega^-, \mathbb{R}^{3 \times 3})$, and $\mu_n, \mu_p \in C^1(\Omega_{\text{Si}}, \mathbb{R}^{3 \times 3})$. For the data, the inclusions $f \in L^\infty(\Omega)$, $V_D \in H^{1/2}(\partial\Omega_D) \cap L^\infty(\Gamma)$, and $u_D, v_D \in H^{1/2}(\partial\Omega_D)$ hold.*

(iii) The doping concentration $C_{\text{dop}}(x)$ is bounded above and below and we define

$$\underline{C} := \inf_{x \in \Omega} C_{\text{dop}}(x) \leq C(x) \leq \sup_{x \in \Omega} C_{\text{dop}}(x) =: \overline{C}.$$

(iv) There is a constant $K \geq 1$ satisfying

$$\frac{1}{K} \leq u_D(x), v_D(x) \leq K \quad \forall x \in \partial\Omega_D.$$

(v) The microscopic models M_α and M_γ depend continuously in $H^1(\Omega)$ on the potential V , and for every potential V in $H^1(\Omega) \cap L^\infty(\Omega)$, the inclusions $\alpha(y) = M_\alpha(V) \in H^{1/2}(\Gamma) \cap L^\infty(\Gamma)$ and $\gamma(y) = M_\gamma(V) \in L^\infty(\Gamma)$ hold.

Using these assumptions, we can state the main result.

THEOREM 2.2 (Existence). *Under Assumptions 2.1, there exists a solution*

$$(V, u, v, \alpha, \gamma) \in (H^1(\Omega \setminus \Gamma) \cap L^\infty(\Omega \setminus \Gamma)) \times (H^1(\Omega_{\text{Si}}) \cap L^\infty(\Omega_{\text{Si}}))^2 \times (H^1(\Gamma) \cap L^\infty(\Gamma))^2$$

of the boundary-value problem (2.4), and it satisfies the L^∞ -estimate

$$\begin{aligned} \frac{1}{K} &\leq u(x) \leq K && \text{in } \Omega_{\text{Si}}, \\ \frac{1}{K} &\leq v(x) \leq K && \text{in } \Omega_{\text{Si}}, \\ \underline{V} &\leq V(x) \leq \overline{V} && \text{in } \Omega, \end{aligned}$$

where

$$\begin{aligned} \underline{V} &:= \min \left(\inf_{\partial\Omega_D} V_D, \Phi - \sup_{\Omega} V_L, U_T \ln \left(\frac{1}{2Kn_i} \left(\underline{C} + \sqrt{\underline{C}^2 + 4n_i^2} \right) \right) - \sup_{\Omega} V_L \right), \\ \overline{V} &:= \max \left(\sup_{\partial\Omega_D} V_D, \Phi - \inf_{\Omega} V_L, U_T \ln \left(\frac{K}{2n_i} \left(\overline{C} + \sqrt{\overline{C}^2 + 4n_i^2} \right) \right) - \inf_{\Omega} V_L \right), \end{aligned}$$

and where V_L is the solution of the linear equation in Lemma 3.1, for which the estimate

$$\|V_L\|_{H^1(\Omega)} \leq C(\|\gamma\|_{L^2(\Gamma)} + \|V_D\|_{H^{1/2}(\partial\Omega)} + \|\alpha\|_{H^{1/2}(\Gamma)})$$

holds.

The existence of solutions will be shown by applying the Schauder fixed-point theorem similarly to [16] for the drift-diffusion equations. It is also known that solutions of the nonlinear Poisson-Boltzmann equation exist. The main issue of our model is how to treat the different equations on a single domain and how the interface conditions (2.1c) and (2.1d) influence estimates of the solutions. As aforementioned, the interface conditions are jumps in the potential V and in the field $-\partial_x V$. The size of the jumps depends on the values of α and γ ; large values of α or γ result in large absolute values of the potential. The influence of the interface conditions on semilinear elliptic problems will be discussed in the following section. Based on the lemmata in the following section, the main result will be proved in Section 4.

3. Semilinear problems including interface conditions

In the proof of the existence result, we will need two lemmata. The first one is concerned with linear elliptic problems with jumps of the form (2.1) and the second one yields the existence and uniqueness of a solution of semilinear elliptic problems including jumps. An a-priori estimate is provided as well.

In the following, $\Gamma \subset \mathbb{R}^d$ will be a C^2 hypersurface in the domain Ω which splits the domain and its boundary into two parts Ω^+ and Ω^- . Here, for the sake of notational simplicity, we denote the one-dimensional coordinate orthogonal to Γ by x and the remaining $(d-1)$ -dimensional coordinates by y . Consequently, the notation $u(0+, y)$ means the limit within Ω^+ and $u(0-, y)$ is the corresponding limit within Ω^- . Furthermore, the jump conditions α and γ depend only on the spatial variable y and not on the potential V as it arises in the iterative structure of the proof of Theorem 2.2. The Dirichlet part of the boundary is denoted by $\partial\Omega_D$ and the Neumann part by $\partial\Omega_N$.

LEMMA 3.1 (Elliptic boundary-value problems with interface conditions). *Assume that $\Omega \subset \mathbb{R}^d$ is a bounded domain with a C^2 boundary split into two nonempty domains Ω^+ and Ω^- by the C^2 hypersurface Γ so that $\text{meas}(\Gamma \cap \partial\Omega) = 0$. Suppose that A with $A|_{\Omega^+} \in C^1(\Omega^+, \mathbb{R}^{d \times d})$ and $A|_{\Omega^-} \in C^1(\Omega^-, \mathbb{R}^{d \times d})$ is uniformly elliptic and that $\alpha \in H^{1/2}(\Gamma)$, $\gamma \in L^2(\Gamma)$, $f \in L^2(\Omega)$, and $u_D \in H^{1/2}(\partial\Omega_D)$ hold. Suppose further that $\partial\Omega \cap \Gamma \subset \partial\Omega_N$ holds or that the jump α is compatible with the Dirichlet boundary conditions u_D , i.e., $u_D(0+) - u_D(0-) = \alpha$ holds on $\partial\Omega_D$.*

Then the boundary-value problem with interface conditions

$$\begin{aligned} -\nabla \cdot (A(x)\nabla u) &= f && \text{in } \Omega \setminus \Gamma, \\ u(0+, y) - u(0-, y) &= \alpha && \text{on } \Gamma, \\ A(0+)\partial_x u(0+, y) - A(0-)\partial_x u(0-, y) &= \gamma && \text{on } \Gamma, \\ \nabla_\nu u &= 0 && \text{on } \partial\Omega_N, \\ u &= u_D && \text{on } \partial\Omega_D \end{aligned}$$

has a unique solution $u \in L^2(\Omega)$ and $u|_{\Omega^+} \in H^1(\Omega^+)$ and $u|_{\Omega^-} \in H^1(\Omega^-)$ hold. Furthermore, the estimate

$$\|u\|_{H^1(\Omega^+)} + \|u\|_{H^1(\Omega^-)} \leq C(\|f\|_{L^2(\Omega)} + \|\gamma\|_{L^2(\Gamma)} + \|u_D\|_{H^{1/2}(\partial\Omega)} + \|\alpha\|_{H^{1/2}(\Gamma)})$$

holds.

Proof. We extend $\alpha \in H^{1/2}(\Gamma)$ to $\bar{\alpha} \in L^2(\bar{\Omega})$ so that $\bar{\alpha}|_\Gamma = \alpha$, $\bar{\alpha}|_{\Omega^-} = 0$, $\bar{\alpha}|_{\Gamma \cup \Omega^+} \in H^1(\Gamma \cup \Omega^+)$, $\bar{\alpha}|_{\partial\Omega_D} = 0$, and $(\nabla_\nu \bar{\alpha})|_{\partial\Omega_N} = 0$. Such an extension $\bar{\alpha}$ can always be found by solving, e.g., the Laplace equation, since the boundary conditions are smooth enough. Similarly, we extend $u_D \in H^{1/2}(\partial\Omega)$ to $\bar{u}_D \in H^1(\Omega)$. We define

$$w := u - \bar{u}_D - \bar{\alpha}$$

so that the first interface condition becomes $w(0+) - w(0-) = 0$ and the Dirichlet boundary conditions become homogeneous.

Multiplication by test functions v with $v|_{\Omega^+} \in H^1(\Omega^+)$, $v|_{\Omega^-} \in H^1(\Omega^-)$, and $v|_{\partial\Omega} = 0$ and integration by parts on Ω^+ and Ω^- yields the weak formulation for $w \in H_0^1(\Omega)$ as

$$\langle A\nabla w, \nabla v \rangle = \langle f, v \rangle + \int_\Gamma \gamma v ds - \langle A\nabla(\bar{u}_D + \bar{\alpha}), \nabla v \rangle,$$

where $\langle \cdot, \cdot \rangle$ denotes the scalar product $\langle f, g \rangle := \int_{\Omega^+} fg + \int_{\Omega^-} fg$ and where we have used the identity

$$\int_{\Gamma} A(0+) \partial_x u(0+, y) v dy - \int_{\Gamma} A(0-) \partial_x u(0-, y) v dy = \int_{\Gamma} \gamma v dy.$$

Since the right-hand side of the weak formulation is a bounded functional, the Lax-Milgram Theorem yields the assertion.

The extensions \bar{u}_D and $\bar{\alpha}$ are not unique. Therefore the uniqueness of the solution u must be shown as well. Suppose u_1 and u_2 are two solutions. We define $u := u_1 - u_2$ and find that u solves the homogeneous problem

$$\begin{aligned} -\nabla \cdot (A(x) \nabla u) &= 0 && \text{in } \Omega \setminus \Gamma, \\ u(0+, y) - u(0-, y) &= 0 && \text{on } \Gamma, \\ A(0+) \partial_x u(0+, y) - A(0-) \partial_x u(0-, y) &= 0 && \text{on } \Gamma, \\ \nabla_{\nu} u &= 0 && \text{on } \partial\Omega_N, \\ u &= 0 && \text{on } \partial\Omega_D, \end{aligned}$$

and hence the maximum principle yields $u = u_1 - u_2 = 0$ almost everywhere.

Finally, we show the estimate. The definition of w yields

$$\begin{aligned} \|u\|_{H^1(\Omega^+)} &\leq \|w\|_{H^1(\Omega^+)} + \|\bar{u}_D\|_{H^1(\Omega^+)} + \|\bar{\alpha}\|_{H^1(\Omega^+)}, \\ \|u\|_{H^1(\Omega^-)} &\leq \|w\|_{H^1(\Omega^-)} + \|\bar{u}_D\|_{H^1(\Omega^-)} + \|\bar{\alpha}\|_{H^1(\Omega^-)}. \end{aligned}$$

Substituting $v = w$ in the weak formulation and using the uniform ellipticity of A , we obtain

$$\begin{aligned} \|w\|_{H^1(\Omega^+)} + \|w\|_{H^1(\Omega^-)} &\leq C(\|f\|_{L^2(\Omega^+)} + \|f\|_{L^2(\Omega^-)} + \|\gamma\|_{L^2(\Gamma)} \\ &\quad + \|\bar{u}_D\|_{H^1(\Omega^+)} + \|\bar{\alpha}\|_{H^1(\Omega^+)} + \|\bar{u}_D\|_{H^1(\Omega^-)} + \|\bar{\alpha}\|_{H^1(\Omega^-)}). \end{aligned}$$

Combining these inequalities and using the inequality $\|\bar{\phi}\|_{H^1(\Omega)} \leq C\|\phi\|_{H^{1/2}(\partial\Omega)}$ [23] yields the asserted estimate. (Note that C denotes a general constant.) \square

The estimate allows a physical interpretation. The value γ corresponds to the presence of charges; therefore f and γ are present in the estimate analogously in the same norm as $\|f\|_{L^2(\Omega)}$ and $\|\gamma\|_{L^2(\Gamma)}$, respectively. The value α corresponds to a dipole moment and results in a shift or jump of the potential; this is similar to a Dirichlet boundary condition and hence α and u_D appear as $\|\alpha\|_{H^{1/2}(\Gamma)}$ and $\|u_D\|_{H^{1/2}(\partial\Omega)}$ in the same norm. This means that the terms on the right-hand side of the estimate are consistent with the physical meaning of the problem.

If in Lemma 3.1 the data α , γ , f , and u_D are bounded, then the solution u is bounded as well, i.e., $u \in L^\infty(\Omega)$ (see, e.g., [24]).

Having treated the linear problem with interface conditions, we now consider the semilinear problem with interface conditions

$$-\nabla \cdot (A(x) \nabla u) + g(x, u) = f \quad \text{in } \Omega \setminus \Gamma, \tag{3.1a}$$

$$u(0+, y) - u(0-, y) = \alpha \quad \text{on } \Gamma, \tag{3.1b}$$

$$A(0+) \partial_x u(0+, y) - A(0-) \partial_x u(0-, y) = \gamma \quad \text{on } \Gamma, \tag{3.1c}$$

$$\nabla_{\nu} u = 0 \quad \text{on } \partial\Omega_N, \tag{3.1d}$$

$$u = u_D \quad \text{on } \partial\Omega_D. \tag{3.1e}$$

We split the solution u into the solution u_L of a linear problem and the solution u_N of a nonlinear problem so that

$$u = u_L + u_N,$$

where u_L is the solution of the problem in Lemma 3.1 and u_N is the solution of the boundary-value problem

$$-\nabla \cdot (A(x)\nabla u_N) + g(x, u_L + u_N) = 0 \quad \text{in } \Omega, \tag{3.2a}$$

$$\nabla_\nu u_N = 0 \quad \text{on } \partial\Omega_N, \tag{3.2b}$$

$$u_N = u_D \quad \text{on } \partial\Omega_D, \tag{3.2c}$$

which is treated in the following lemma. The use of the Leray-Schauder fixed-point theorem is similar to [16].

LEMMA 3.2 (Semilinear elliptic boundary-value problems with interface conditions). *Suppose that $\Omega, \Gamma, A, f, u_D, \alpha,$ and γ are as in Lemma 3.1 and additionally that $f, u_D, \alpha,$ and γ are bounded. Suppose further*

(i) *that the function $g(x, u) \in C^1(\Omega \times \mathbb{R})$ is monotonically increasing in u for all $x \in \Omega,$*

(ii) *that there exist functions $\underline{g}(u)$ and $\tilde{g}(u)$ so that*

$$\underline{g}(u) \leq g(x, u) \leq \tilde{g}(u) \quad \forall x \in \Omega \quad \forall u, \quad \text{and}$$

(iii) *that the algebraic equations $\underline{g}(\tilde{u}) = 0$ and $\tilde{g}(\underline{u}) = 0$ have solutions.*

Then there exists a unique solution $u = u_L + u_N$ of the semilinear elliptic boundary-value problem with interface conditions (3.1) and $u_N \in H^1(\Omega) \cap L^\infty(\Omega)$ holds. Furthermore, the solution u_N satisfies the estimate

$$\kappa \leq u_N(x) \leq \lambda \quad \forall x \in \bar{\Omega},$$

where

$$\tilde{\kappa} := \arg \max_z (g(x, z + \sup_\Omega u_L) \leq 0 \quad \forall x \in \Omega),$$

$$\kappa := \min(\tilde{\kappa}, \inf_{\partial\Omega} u_D),$$

$$\tilde{\lambda} := \arg \min_z (g(x, z + \inf_\Omega u_L) \geq 0 \quad \forall x \in \Omega),$$

$$\lambda := \max(\tilde{\lambda}, \sup_{\partial\Omega} u_D).$$

Proof. 1. To show the existence and uniqueness, we use a fixed-point theorem and a maximum principle. First, for the uniqueness of the solution, we assume that there are two weak solutions $u_1, u_2 \in H^1(\Omega) \cap L^\infty(\Omega).$ We set $w := u_1 - u_2$ and find

$$\begin{aligned} -\nabla \cdot (A(x)\nabla w) + g(x, u_1) - g(x, u_2) &= 0 \quad \text{in } \Omega, \\ \nabla_\nu w &= 0 \quad \text{on } \partial\Omega_N, \\ w &= 0 \quad \text{on } \partial\Omega_D \end{aligned}$$

with

$$-\nabla \cdot (A(x)\nabla w) + g(x, u_1) - g(x, u_2) = -\nabla \cdot (A(x)\nabla w) + \partial_w g(x, \hat{w}(x))w = 0,$$

using the mean-value theorem to find $\hat{w}(x)$. Since $\partial_u g(x, \hat{w}(x)) \geq 0$ by assumption, we can use the maximum principle to conclude that $w = 0$ a.e. Hence the two solutions are identical a.e.

2. To show the estimate $\kappa \leq u_N \leq \lambda$, we use a cut-off argument similar to [15, 25]. Suppose that u_N is a solution. We start by defining

$$\begin{aligned} \underline{u} &:= (u_N - \kappa)^- = \min(u_N - \kappa, 0), \\ \bar{u} &:= (u_N - \lambda)^+ = \max(u_N - \lambda, 0). \end{aligned}$$

Clearly $\underline{u}, \bar{u} \in H_0^1(\Omega)$, since $u_N \in H^1(\Omega)$. The weak formulation of the problem (3.2) is

$$\langle A \nabla u_N, \nabla v \rangle + \langle g(x, u_L + u_N), v \rangle = 0 \quad \forall v \in H^1(\Omega),$$

and we will be able to use \underline{u} and \bar{u} as test functions in this equation.

Next, we estimate g on the support of \underline{u} and \bar{u} . The support of \underline{u} is $\text{supp } \underline{u} = \{x \in \bar{\Omega} \mid u_N(x) \leq \kappa\}$ and the support of \bar{u} is $\text{supp } \bar{u} = \{x \in \bar{\Omega} \mid u_N(x) \geq \lambda\}$. By the definitions of $\tilde{\kappa}$ and $\tilde{\lambda}$ and the monotonicity of g , we obtain

$$\begin{aligned} g(x, u_N + u_L) &\leq g(x, \tilde{\kappa}) \leq 0 \quad \forall x \in \text{supp } \underline{u}, \\ g(x, u_N + u_L) &\geq g(x, \tilde{\lambda}) \geq 0 \quad \forall x \in \text{supp } \bar{u}. \end{aligned}$$

Due to the last two inequalities, the fact that $\underline{u} \leq 0$ and $\bar{u} \geq 0$ in $\bar{\Omega}$, and using the uniform ellipticity of A with constant C , we deduce from the weak formulation that

$$\begin{aligned} 0 &\geq \langle A \nabla u_N, \nabla \underline{u} \rangle = \langle A \nabla (u_N - \kappa), \nabla \underline{u} \rangle = \langle A \nabla (u_N - \kappa)^-, \nabla \underline{u} \rangle = \langle A \nabla \underline{u}, \nabla \underline{u} \rangle \\ &\geq C \|\nabla \underline{u}\|_{L^2(\Omega)}^2 \geq 0, \end{aligned}$$

and analogously

$$\begin{aligned} 0 &\geq \langle A \nabla u_N, \nabla \bar{u} \rangle = \langle A \nabla (u_N - \lambda), \nabla \bar{u} \rangle = \langle A \nabla (u_N - \lambda)^+, \nabla \bar{u} \rangle = \langle A \nabla \bar{u}, \nabla \bar{u} \rangle \\ &\geq C \|\nabla \bar{u}\|_{L^2(\Omega)}^2 \geq 0. \end{aligned}$$

Therefore $\|\nabla \underline{u}\|_{L^2(\Omega)} = 0$ and $\|\nabla \bar{u}\|_{L^2(\Omega)} = 0$ hold. Using the Poincaré inequalities $\|\underline{u}\|_{L^2} \leq C \|\nabla \underline{u}\|_{L^2}$ and $\|\bar{u}\|_{L^2} \leq C \|\nabla \bar{u}\|_{L^2}$, we find $\underline{u} = 0$ and $\bar{u} = 0$ a.e., which yields the asserted estimate.

3. To prove the existence of a solution, we define the cut function

$$v^K(x) := \begin{cases} K, & \text{if } K \leq v(x), \\ v(x), & \text{if } -K \leq v(x) \leq K, \\ -K, & \text{if } v(x) \leq -K \end{cases}$$

for $v \in L^2(\Omega)$. Obviously, we have $v^K \in L^\infty(\Omega)$. Since u_N is bounded by the estimate in the previous step, K can be chosen large enough so that $u_N = u_N^K$.

Next, we define the operator

$$M: L^2(\Omega) \times [0, 1] \rightarrow L^2(\Omega)$$

by $M(v, \sigma) = w$, where w is the solution of the boundary-value problem

$$\begin{aligned} -\nabla \cdot (A \nabla w) + \sigma g(x, u_L + v^K) &= 0 && \text{in } \Omega, \\ w &= \sigma u_D && \text{on } \partial \Omega_D, \\ \nabla_\nu w &= 0 && \text{on } \partial \Omega_N. \end{aligned}$$

Every fixed point of $M(., 1)$ is a solution of the semilinear problem (3.2). Due to the estimate shown in the previous step, K can be chosen large enough so that $-K \leq w \leq K$ holds a.e. in Ω for every fixed point $w = M(w, 1)$.

To apply the Leray-Schauder fixed-point theorem, the compactness of M must be shown. The continuity of M follows from the continuity of the cut function, the continuous dependence of $\sigma g(x, u_L + v^K)$ on $(v, \sigma) \in L^2(\Omega) \times [0, 1]$, and the continuous dependence of the H^1 solutions of elliptic equations on $L^2(\Omega)$ right-hand sides and H^1 boundary data. Furthermore, the range of M is bounded with respect to the H^1 norm, since w is the solution of a linear elliptic equation with the inhomogeneity $g(x, u_L + v^K)$ that is bounded because g is bounded as a function of x and both u_L and v^K are bounded, i.e., the inequality

$$\begin{aligned} \|w\|_{H^1(\Omega)} &\leq C(\|\sigma g(., u_L + v^K)\|_{L^2(\Omega)} + \|\sigma u_D\|_{H^{1/2}(\partial\Omega)}) \\ &\leq C(|\Omega|^{1/2} \sup_{x \in \bar{\Omega}} |g(x, u_L + v^K)| + \|u_D\|_{H^{1/2}(\partial\Omega)}) \end{aligned}$$

holds. We know that $H^1(\Omega)$ is compactly embedded in $L^2(\Omega)$ due to the Rellich-Kondrachov compactness theorem. Since the range of M is bounded, the operator M is compact.

Finally, the Leray-Schauder fixed-point theorem yields the existence of a fixed point w of $M(., 1)$ and hence the existence of a solution u_N of the original boundary-value problem. □

4. Proof of Theorem 2.2

The following proof of Theorem 2.2 is based on the Schauder fixed-point theorem and the estimates are deduced from a maximum principle (see Lemma 3.2). The main idea of the proof follows [15], while the emphasis is on the different fixed-point map and the different estimates.

1. We start by defining the map $G: N \rightarrow N$, which will be shown to satisfy the assumptions of the fixed-point theorem, where

$$\begin{aligned} N := \{ &(V, u, v, \alpha, \gamma) \in L^2(\Omega) \times L^2(\Omega_{Si})^2 \times L^2(\Gamma)^2 \mid \underline{V} \leq V(x) \leq \bar{V} \text{ a.e. in } \Omega, \\ &\frac{1}{K} \leq u(x), v(x) \leq K \text{ a.e. in } \Omega_{Si}, \quad \alpha, \gamma \text{ bounded a.e. on } \Gamma \} \end{aligned}$$

and $(V_1, u_1, v_1, \alpha_1, \gamma_1) = G((V_0, u_0, v_0, \alpha_0, \gamma_0))$, as follows.

(i) Solve the boundary-value problem with interface conditions

$$-\nabla \cdot (A \nabla V_1) = \begin{cases} qC_{\text{dop}} - qn_i(e^{V_1/U_T} u_0 - e^{-V_1/U_T} v_0) & \text{in } \Omega_{Si}, \\ 0 & \text{in } \Omega_{\text{ox}}, \\ -2\eta \sinh(\beta(V_1 - \Phi)) & \text{in } \Omega_{\text{liq}}, \end{cases} \quad (4.1a)$$

$$V_1(0+, y) - V_1(0-, y) = \alpha_0(y) \quad \text{on } \Gamma, \quad (4.1b)$$

$$A(0+) \partial_x V_1(0+, y) - A(0-) \partial_x V_1(0-, y) = \gamma_0(y) \quad \text{on } \Gamma, \quad (4.1c)$$

$$V_1 = V_D \quad \text{on } \partial\Omega_D, \quad (4.1d)$$

$$\nabla_\nu V_1 = 0 \quad \text{on } \partial\Omega_N \quad (4.1e)$$

for V_1 .

(ii) Solve the elliptic boundary-value problem

$$U_T n_i \nabla \cdot (\mu_n e^{V_1/U_T} \nabla u_1) - n_i \frac{u_1 v_0 - 1}{\tau_p(e^{V_1/U_T} u_0 + 1) + \tau_n(e^{-V_1/U_T} v_0 + 1)} = 0 \quad \text{in } \Omega_{Si}, \tag{4.2a}$$

$$u_1 = u_D \quad \text{on } \partial\Omega_D, \tag{4.2b}$$

$$\nabla_\nu u_1 = 0 \quad \text{on } \partial\Omega_N \tag{4.2c}$$

for u_1 .

(iii) Solve the elliptic problem

$$U_T n_i \nabla \cdot (\mu_p e^{-V_1/U_T} \nabla v_1) - n_i \frac{u_0 v_1 - 1}{\tau_p(e^{V_1/U_T} u_0 + 1) + \tau_n(e^{-V_1/U_T} v_0 + 1)} = 0 \quad \text{in } \Omega_{Si}, \tag{4.3a}$$

$$v_1 = v_D \quad \text{on } \partial\Omega_D, \tag{4.3b}$$

$$\nabla_\nu v_1 = 0 \quad \text{on } \partial\Omega_N \tag{4.3c}$$

for v_1 .

(iv) Update the surface-charge density and dipole-moment density according to the microscopic model as

$$\alpha_1(y) := M_\alpha(V_1), \tag{4.4a}$$

$$\gamma_1(y) := M_\gamma(V_1). \tag{4.4b}$$

We show that these three boundary-value problems have unique solutions and that $(V_1, u_1, v_1, \alpha_1, \gamma_1) \in N$, so that the map G is well-defined. The three problems above can be written in the general form considered in Lemma 3.2 and the first problem (4.1) includes interface conditions. The coefficient A in the lemma equals either A , $\mu_n e^{V_1/U_T}$, or $\mu_p e^{-V_1/U_T}$ and hence the equations are uniformly elliptic. In all three cases, $g(x, w)$ is a monotone increasing function of w provided that u_0 and v_0 are positive.

Choose $(V, u_0, v_0, \alpha_0, \gamma_0) \in N$. Lemma 3.2 shows that the first problem (4.1) in the definition of G has a unique solution V_1 . To get the estimates, we first set

$$\underline{g}(V_1) := \min(2\eta \sinh(\beta(V_1 - \Phi)), qn_i (\frac{1}{K} e^{V_1/U_T} - K e^{-V_1/U_T}) - q\bar{C}),$$

$$\tilde{g}(V_1) := \max(2\eta \sinh(\beta(V_1 - \Phi)), qn_i (K e^{V_1/U_T} - \frac{1}{K} e^{-V_1/U_T}) - q\underline{C}).$$

Note that both \underline{g} and \tilde{g} satisfy the requirements of Lemma 3.2. Solving the two algebraic equations

$$\tilde{g}(\tilde{\kappa} + \sup_\Omega V_L) = 0,$$

$$\underline{g}(\tilde{\lambda} + \inf_\Omega V_L) = 0,$$

where V_L is the solution of the linear boundary-value problem of Lemma 3.1, yields

$$\tilde{\kappa} + \sup_\Omega V_L = \min\left(\Phi, U_T \ln\left(\frac{1}{2Kn_i} \left(\underline{C} + \sqrt{\underline{C}^2 + 4n_i^2}\right)\right)\right),$$

$$\tilde{\lambda} + \inf_\Omega V_L = \max\left(\Phi, U_T \ln\left(\frac{K}{2n_i} \left(\bar{C} + \sqrt{\bar{C}^2 + 4n_i^2}\right)\right)\right).$$

Hence we obtain the estimate

$$\begin{aligned}
 V(x) &\geq \min \left(\inf_{\partial\Omega_D} V_D, \Phi - \sup_{\Omega} V_L, U_T \ln \left(\frac{1}{2Kn_i} \left(C + \sqrt{C^2 + 4n_i^2} \right) \right) - \sup_{\Omega} V_L \right), \\
 V(x) &\leq \max \left(\sup_{\partial\Omega_D} V_D, \Phi - \inf_{\Omega} V_L, U_T \ln \left(\frac{K}{2n_i} \left(\bar{C} + \sqrt{\bar{C}^2 + 4n_i^2} \right) \right) - \inf_{\Omega} V_L \right)
 \end{aligned}$$

for all $x \in \Omega$ from Lemma 3.2.

Next, we apply Lemma 3.2 to the second problem (4.2) to find a unique solution u_1 . Here we choose

$$\begin{aligned}
 \underline{g}(u_1) &:= \frac{\frac{1}{K}u_1 - 1}{\tau_p(K e^{\bar{V}/U_T} + 1) + \tau_n(K e^{-\bar{V}/U_T} + 1)}, \\
 \tilde{g}(u_1) &:= \frac{Ku_1 - 1}{\tau_p(\frac{1}{K}e^{\underline{V}/U_T} + 1) + \tau_n(\frac{1}{K}e^{-\underline{V}/U_T} + 1)}.
 \end{aligned}$$

The equation $\underline{g}(\tilde{u}_1) = 0$ yields $\tilde{u}_1 = K$ and the equation $\tilde{g}(u_1) = 0$ yields $u_1 = 1/K$.

The third problem (4.3) is treated analogously and we find unique solutions u_1 and v_1 with the estimates $1/K \leq u_1(x) \leq K$ and $1/K \leq v_1 \leq K$ on Ω_{Si} . Hence G maps N into itself. Note that N is a closed and convex subset of $L^2(\Omega) \times L^2(\Omega_{Si})^2 \times L^2(\Gamma)^2$.

2. We now show that G is continuous. The continuous dependence of the solution V_1 of the first problem (4.1) in the definition of G on the data is obtained from the estimate in Lemma 3.2 and the continuity of the right-hand side in (4.1a). The second problem (4.2) and the third problem (4.3) in the definition of G are special cases of the first. In the fourth problem (4.4), α_1 and γ_1 depend continuously on α_0 and γ_0 due to the continuous dependence of V_1 and the continuity of M_α and M_γ . Therefore G is continuous.

3. The continuous dependence of $(V_1, u_1, v_1, \alpha_1, \gamma_1)$ on the data of the three problems (4.1), (4.2), and (4.3) implies that there is a positive and continuous function F such that

$$\begin{aligned}
 &\|V_1\|_{H^1(\Omega)} + \|u_1\|_{H^1(\Omega_{Si})} + \|v_1\|_{H^1(\Omega_{Si})} \\
 &\leq F(\|C_{\text{dop}}\|_{L^2(\Omega)}, \|V_D\|_{H^1(\partial\Omega)}, \|u_D\|_{H^1(\partial\Omega_{Si})}, \|v_D\|_{H^1(\partial\Omega_{Si})}, \|\alpha_0\|_{H^{1/2}(\Gamma)}, \|\gamma_0\|_{L^2(\Gamma)}).
 \end{aligned}$$

Hence we find for $(V_0, u_0, v_0, \alpha_0, \gamma_0) \in N$ that the inequality

$$\|V_1\|_{H^1(\Omega)} + \|u_1\|_{H^1(\Omega_{Si})} + \|v_1\|_{H^1(\Omega_{Si})} \leq C$$

holds for a constant C . Furthermore, $\|\alpha_1\|_{H^1(\Gamma)}$ and $\|\gamma_1\|_{H^1(\Gamma)}$ are bounded due to the assumptions on M_α and M_γ .

This yields that the image $G(N)$, consisting of all $(V_1, u_1, v_1, \alpha_1, \gamma_1)$, is bounded as a subset of $H^1(\Omega) \times H^1(\Omega_{Si})^2 \times H^1(\Gamma)^2$. Now the Rellich-Kondrachov compactness theorem implies that the image $G(N)$ is precompact in $L^2(\Omega) \times L^2(\Omega_{Si})^2 \times L^2(\Gamma)^2$.

4. In summary, all the assumptions of the Schauder fixed-point theorem are satisfied and hence we obtain the existence of a fixed-point of G , i.e., the existence of a weak solution of the original problem. □

5. Local uniqueness

In general, the solution in Theorem 2.2 is not unique. Recalling the derivation of the drift-diffusion equations from the Boltzmann transport equation, it is clear that the drift-diffusion equations implicitly assume that the particle velocities are distributed according to a Maxwellian distribution, i.e., they are in thermal equilibrium. However, large applied voltages and correspondingly large currents result in fast particles for which Maxwellian distributions centered at $v=0$ are certainly not adequate.

Uniqueness of the solution therefore holds only in a neighborhood around thermal equilibrium with respect to the Dirichlet boundary conditions. Thermal equilibrium is the solution where the fluxes J_n and J_p in the semiconductor vanish, where the fluxes of the ions and molecules into and out of the boundary layer at the sensor surface vanish as well, i.e., the surface reactions have reached the equilibrium state, and where the voltages $U \in \mathbb{R}^k$, that are applied at each of the k contacts that constitute $\partial\Omega_D$, are equal to the Fermi level.

The equilibrium potential is called V_e and the equilibrium surface densities are called α_e and γ_e ; the equilibrium potential is then the solution of the equilibrium boundary-value problem

$$-\nabla \cdot (A \nabla V_e) = qC_{\text{dop}} - qn_i(e^{V_e/U_T} - e^{-V_e/U_T}) \quad \text{in } \Omega_{\text{Si}}, \tag{5.1a}$$

$$-\nabla \cdot (A \nabla V_e) = 0 \quad \text{in } \Omega_{\text{ox}}, \tag{5.1b}$$

$$-\nabla \cdot (A \nabla V_e) = -2\eta \sinh(\beta(V_e - \Phi)) \quad \text{in } \Omega_{\text{liq}}, \tag{5.1c}$$

$$V_e(0+, y) - V_e(0-, y) = \alpha_e \quad \text{on } \Gamma, \tag{5.1d}$$

$$A(0+)\partial_x V_e(0+, y) - A(0-)\partial_x V_e(0-, y) = \gamma_e \quad \text{on } \Gamma, \tag{5.1e}$$

$$V_e = V_D(0) \quad \text{on } \partial\Omega_D, \tag{5.1f}$$

$$\nabla_\nu V_e = 0 \quad \text{on } \partial\Omega_N, \tag{5.1g}$$

and it exists uniquely due to Lemma 3.2.

In order to state the uniqueness result, we need the following assumptions on the data.

ASSUMPTIONS 5.1.

(i) The recombination rate R has the form $R = F(x, V, u, v)(uv - 1)$, where $F(x, \dots) \in C^2(\mathbb{R} \times \mathbb{R}_+^2)$ holds for all $x \in \Omega$ and where the derivatives $\partial_{(V, u, v)}^\beta F(\cdot, V, u, v)$ are in $L^\infty(\Omega)$ uniformly for all (V, u, v) in bounded subsets of $\mathbb{R} \times \mathbb{R}_+^2$ and for all multiindices β with $|\beta| \leq 2$.

Furthermore, there are constants $\underline{\omega}$ and $\bar{\omega}$ such that either $0 < \underline{\omega} \leq F(x, V_e(x), 1, 1) \leq \bar{\omega}$ or $F(x, V_e(x), 1, 1) = 0$ holds for all $x \in \Omega$.

(ii) The Dirichlet data (V_D, u_D, v_D) are a Lipschitz-continuously differentiable map of U from \mathbb{R}^k into $H^2(\Omega) \times H^2(\Omega_{\text{Si}})^2$ and $u_D(0) = v_D(0) = 1$ holds in Ω_{Si} .

(iii) The solution u of the boundary-value problem $-\nabla \cdot (A\nabla u) = f$ in Ω , $u = 0$ on $\partial\Omega_D$, and $\nabla_\nu u = 0$ on $\partial\Omega_N$, satisfies the inequality

$$\|u\|_{W^{2,q}(\Omega)} \leq C\|f\|_{L^q(\Omega)}$$

for all $f \in L^q(\Omega)$ with $q = 2$ and $q = 3/2$. This is actually a condition on the boundary segments $\partial\Omega_D$ and $\partial\Omega_N$; it excludes boundaries where Dirichlet and Neumann segments meet under angles larger than $\pi/2$.

(iv) The Fréchet derivatives M'_α and M'_γ of the interface models M_α and M_γ with respect to V exist, they are in $H^{1/2}(\Gamma)$ and $L^2(\Gamma)$, respectively, and they satisfy the inequality

$$\|M'_\alpha(V)\|_{H^{1/2}(\Gamma)} + \|M'_\gamma(V)\|_{L^2(\Gamma)} \leq C\|V\|_{H^2(\Omega)}$$

in a neighborhood of the equilibrium potential V_e with a sufficiently small constant C .

The following theorem yields the local uniqueness of the solution of (2.4). The proof is based on the implicit-function theorem.

THEOREM 5.2 (Local uniqueness). *Under Assumptions 2.1 and 5.1, there exists a sufficiently small $\sigma \in \mathbb{R}$ with $|U| < \sigma$ such that the problem in Theorem 2.2 has a locally unique solution*

$$(V^*(U), u^*(U), v^*(U), \alpha^*(U), \gamma^*(U)) \in H^2(\Omega) \times H^2(\Omega_{\text{Si}})^2 \times H^{1/2}(\Gamma) \times L^2(\Gamma).$$

The solution satisfies

$$(V^*(0), u^*(0), v^*(0), \alpha^*(0), \gamma^*(0)) = (V_e, 1, 1, \alpha_e, \gamma_e)$$

and it depends continuously differentiablely on U as a map from $\{U \in \mathbb{R}^k \mid |U| < \sigma\}$ into $H^2(\Omega) \times H^2(\Omega_{\text{Si}})^2 \times H^{1/2}(\Gamma) \times L^2(\Gamma)$.

Proof. 1. We start with the substitution $\tilde{V} := V - V_D(U)$, $\tilde{u} := u - u_D(U)$, and $\tilde{v} := v - v_D(U)$. For notational simplicity, we denote \tilde{V} , \tilde{u} , and \tilde{v} again by V , u , and v . After the substitution, the system (2.4) becomes

$$\begin{aligned} &-\nabla \cdot (A\nabla(V + V_D)) \\ &\quad = qC_{\text{dop}} - qn_i(e^{(V+V_D)/U_T}u - e^{-(V+V_D)/U_T}v) \quad \text{in } \Omega_{\text{Si}}, \\ &-\nabla \cdot (A\nabla(V + V_D)) = 0 \quad \text{in } \Omega_{\text{ox}}, \\ &-\nabla \cdot (A\nabla(V + V_D)) = -2\eta \sinh(\beta(V + V_D - \Phi)) \quad \text{in } \Omega_{\text{liq}}, \\ &V(0+, y) - V(0-, y) = \alpha \quad \text{on } \Gamma, \\ &A(0+)\partial_x V(0+, y) - A(0-)\partial_x V(0-, y) = \gamma \quad \text{on } \Gamma, \\ &U_T n_i \nabla \cdot (\mu_n e^{(V+V_D)/U_T} \nabla(u + u_D)) \\ &\quad = F(x, V + V_D, u + u_D, v + v_D)((u + u_D)(v + v_D) - 1) \quad \text{in } \Omega_{\text{Si}}, \\ &U_T n_i \nabla \cdot (\mu_p e^{-(V+V_D)/U_T} \nabla(v + v_D)) \\ &\quad = F(x, V + V_D, u + u_D, v + v_D)((u + u_D)(v + v_D) - 1) \quad \text{in } \Omega_{\text{Si}}, \\ &\quad \alpha = M_\alpha(V) \quad \text{on } \Gamma, \\ &\quad \gamma = M_\gamma(V) \quad \text{on } \Gamma, \\ &\quad V = 0 \quad \text{on } \partial\Omega_D, \end{aligned}$$

$$\begin{aligned}
 u = v = 0 & && \text{on } \partial\Omega_{D,\text{Si}}, \\
 \nabla_\nu V = 0 & && \text{on } \partial\Omega_N, \\
 \nabla_\nu u = \nabla_\nu v = 0 & && \text{on } \partial\Omega_{N,\text{Si}}.
 \end{aligned}$$

We write this boundary-value problem as the operator equation

$$G(V, u, v, \alpha, \gamma, U) = 0,$$

where the map

$$G: B \times S_{\sigma_1}(0) \rightarrow L^2(\Omega) \times L^2(\Omega_{\text{Si}})^2 \times H^{1/2}(\Gamma) \times L^2(\Gamma) \tag{5.2}$$

is given by the boundary-value problem above. Here B is an open subset of $H^2_\delta(\Omega \setminus \Gamma) \times H^2_\delta(\Omega_{\text{Si}})^2 \times H^{1/2}(\Gamma) \times L^2(\Gamma)$ with

$$H^2_\delta(\Omega) := \{ \phi \in H^2(\Omega) \mid \nabla_\nu \phi = 0 \text{ on } \partial\Omega_N, \quad \phi = 0 \text{ on } \partial\Omega_D \}$$

and the sphere $S_{\sigma_1}(0)$ with radius σ_1 and center 0 is a subset of \mathbb{R}^k . The domain must be chosen such that $u = \tilde{u} + u_D > 0$ and $v = \tilde{v} + v_D > 0$ for all $(V, u, v, \alpha, \gamma) \in B$ and for all $U \in S_{\sigma_1}(0)$, because u and v are positive and the recombination rate R is defined only for positive u and v .

Since $u_D(0) = 1$ (this is the boundary condition for $U = 0$ of the equilibrium solution), we have to ensure that $\|\tilde{u}\|_{L^\infty(\Omega_{\text{Si}})}$ is small enough so that u is positive. To ensure this, we choose B bounded and small enough; if $\|\tilde{u}\|_{H^2(\Omega_{\text{Si}})}$ is small enough, this indeed implies that $\|\tilde{u}\|_{L^\infty(\Omega_{\text{Si}})}$ is small enough due to the inequality $\|u\|_{L^\infty(U)} \leq C\|u\|_{H^2(U)}$ for all $f \in H^2(U)$. The same argument ensures that v is positive if B is bounded and small enough.

Since $G(V, u, v, \alpha, \gamma, U) \in L^2(\Omega) \times L^2(\Omega_{\text{Si}})^2 \times H^{1/2}(\Gamma) \times L^2(\Gamma)$ implies that $(V, u, v, \alpha, \gamma) \in B$ and $U \in S_{\sigma_1}(U)$, and since products of functions in B are in $L^2(\Omega)$ due to the inequality $\|uv\|_{L^2(U)} \leq C\|u\|_{H^1(U)}\|v\|_{H^1(U)}$ for all u and $v \in H^1(U)$, the map G , as stated in (5.2), is well-defined.

2. The equilibrium solution $(V_e - V_D(0), 0, 0, \alpha_e, \gamma_e, 0)$ is obviously a solution of the equation $G = 0$. To apply the implicit-function theorem, the Fréchet derivative

$$D_{(V,u,v,\alpha,\gamma)}G(V_e - V_D(0), 0, 0, \alpha_e, \gamma_e, 0)$$

must have a bounded inverse. To find the inverse of the Fréchet derivative, we solve the equation

$$D_{(V,u,v,\alpha,\gamma)}G(V_e - V_D(0), 0, 0, \alpha_e, \gamma_e, 0)(a_1, a_2, a_3, a_4, a_5) = (g_1, g_2, g_3, g_4, g_5) \tag{5.3}$$

for a_i , where $(g_1, g_2, g_3, g_4, g_5) \in L^2(\Omega) \times L^2(\Omega_{\text{Si}})^2 \times H^{1/2}(\Gamma) \times L^2(\Gamma)$. This equation is

equivalent to the boundary-value problem

$$-\nabla \cdot (A \nabla a_1) = -qn_i \left(\left(\frac{e^{V_e/U_T} + e^{-V_e/U_T}}{U_T} \right) a_1 + e^{-V_e/U_T} a_2 - e^{V_e/U_T} a_3 \right) + g_1 \quad \text{in } \Omega_{\text{Si}}, \quad (5.4a)$$

$$-\nabla \cdot (A \nabla a_1) = g_1 \quad \text{in } \Omega_{\text{ox}}, \quad (5.4b)$$

$$-\nabla \cdot (A \nabla a_1) = -2\eta\beta \sinh(\beta(V_e - \Phi)) a_1 + g_1 \quad \text{in } \Omega_{\text{liq}}, \quad (5.4c)$$

$$a_1(0+, y) - a_1(0-, y) = a_4 \quad \text{on } \Gamma, \quad (5.4d)$$

$$A(0+) \partial_x a_1(0+, y) - A(0-) \partial_x a_1(0-, y) = a_5 \quad \text{on } \Gamma, \quad (5.4e)$$

$$n_i \nabla \cdot (\mu_n e^{V_e/U_T} \nabla a_2) = \omega(x) a_2 + \omega(x) a_3 + g_2 \quad \text{in } \Omega_{\text{Si}}, \quad (5.4f)$$

$$n_i \nabla \cdot (\mu_p e^{-V_e/U_T} \nabla a_3) = \omega(x) a_2 + \omega(x) a_3 + g_3 \quad \text{in } \Omega_{\text{Si}}, \quad (5.4g)$$

$$a_4 = M'_\alpha(V_e) a_1 + g_4 \quad \text{on } \Gamma, \quad (5.4h)$$

$$a_5 = M'_\gamma(V_e) a_1 + g_5 \quad \text{on } \Gamma, \quad (5.4i)$$

$$a_1 = 0 \quad \text{on } \partial\Omega_D, \quad (5.4j)$$

$$a_2 = a_3 = 0 \quad \text{on } \partial\Omega_{D,\text{Si}}, \quad (5.4k)$$

$$\nabla_\nu a_1 = 0 \quad \text{on } \partial\Omega_N, \quad (5.4l)$$

$$\nabla_\nu a_2 = \nabla_\nu a_3 = 0 \quad \text{on } \partial\Omega_{N,\text{Si}}, \quad (5.4m)$$

where $\omega(x) := F(x, V_e(x), 1, 1)$ and either $0 < \underline{\omega} \leq f(x) \leq \bar{\omega}$ or $\omega = 0$ holds in Ω_{Si} due to the assumptions on the recombination rate.

In the case $\omega = 0$ in Ω , the equations (5.4f) and (5.4g) are decoupled from the first equation and from each other. Hence the existence of a unique solution and the boundedness of the inverse are seen immediately.

In the case $0 < \underline{\omega} \leq f(x) \leq \bar{\omega}$ in Ω_{Si} , the unique existence of the solutions a_2 and a_3 of the equations (5.4f) and (5.4g) are shown as in the proof of Theorem 3.3.1 in [15].

In both cases, the estimate

$$\|a_2\|_{H^2(\Omega_{\text{Si}})} + \|a_3\|_{H^2(\Omega_{\text{Si}})} \leq C(\|g_2\|_{L^2(\Omega_{\text{Si}})} + \|g_3\|_{L^2(\Omega_{\text{Si}})})$$

holds.

3. By substituting a_2 and a_3 into (5.4a), we find the estimate

$$\begin{aligned} \|a_1\|_{H^2(\Omega)} \leq C_1(\|g_1\|_{L^2(\Omega)} + \|g_2\|_{L^2(\Omega_{Si})} + \|g_3\|_{L^2(\Omega_{Si})} + \|g_4\|_{H^{1/2}(\Gamma)} + \|g_5\|_{L^2(\Gamma)} \\ + \|a_4\|_{H^{1/2}(\Gamma)} + \|a_5\|_{L^2(\Gamma)}) \end{aligned}$$

using Lemma 3.1. Equations (5.4h) and (5.4i) and Assumption 5.1(iv) on M_α and M_γ yields the existence of a sufficiently small constant C_2 such that the inequality

$$\|a_4\|_{H^{1/2}(\Gamma)} + \|a_5\|_{L^2(\Gamma)} \leq C_2\|a_1\|_{H^2(\Omega)} + \|g_4\|_{H^{1/2}(\Gamma)} + \|g_5\|_{L^2(\Gamma)}$$

holds. For sufficiently small C_2 , i.e., if $C_1C_2 < 1$, the last two inequalities yield

$$\begin{aligned} (1 - C_1C_2)\|a_1\|_{H^2(\Omega)} \leq C_1(\|g_1\|_{L^2(\Omega)} + \|g_2\|_{L^2(\Omega_{Si})} + \|g_3\|_{L^2(\Omega_{Si})} \\ + 2\|g_4\|_{H^{1/2}(\Gamma)} + 2\|g_5\|_{L^2(\Gamma)}). \end{aligned}$$

Hence we have shown that the Fréchet derivative has a bounded inverse, i.e., there is a constant C such that the inequality

$$\|(D_{(V,u,v,\alpha,\gamma)}G(V_e - V_D(0), 0, 0, \alpha_e, \gamma_e, 0))^{-1}\| \leq C$$

holds, where the norm is the operator norm of

$$L^2(\Omega) \times L^2(\Omega_{Si})^2 \times H^{1/2}(\Gamma) \times L^2(\Gamma) \rightarrow H^2(\Omega \setminus \Gamma) \times H^2(\Omega_{Si})^2 \times H^{1/2}(\Gamma) \times L^2(\Gamma).$$

Finally, the implicit-function theorem yields the assertion. □

6. Discretization

In order to calculate numerical solutions of the model equations (2.4), the system was discretized using a finite-volume Scharfetter-Gummel method, where the microscopic models yielding surface charge and dipole moment are treated as an additional step in its iterative scheme. To discretize the Poisson equation, special care has to be taken at the interface Γ . At Γ , two grid points are placed with identical coordinates corresponding to the two limit values $V(0+)$ and $V(0-)$. When Γ is parallel to the y -coordinates, we denote the two limit values as $V_{i+1,j,k}$ and $V_{i,j,k}$ and the two interface conditions (2.4d) and (2.4e) become the two discretized equations

$$V_{i+1,j,k} - V_{i,j,k} = \alpha, \tag{6.1a}$$

$$A(0+) \frac{V_{i+2,j,k} - V_{i+1,j,k}}{\Delta x} - A(0-) \frac{V_{i,j,k} - V_{i-1,j,k}}{\Delta x} = \gamma, \tag{6.1b}$$

where Δx is the grid spacing in x -direction.

The numbering of the additional grid points at the interface is crucial to obtain a system matrix with a small bandwidth. If the grid points are numbered in a naive way, the typical bandwidth structure of discretized Laplace-type operators is lost. In order to arrive at a numbering scheme for the grid points which allows to implement the interface conditions efficiently, it is advantageous to first associate the variables $V_{i,j,k}$ with the potential values on an equidistant grid (see Figure 6.1) and then to relate the variables $V_{i,j,k}$ in the vicinity of the interface according to the equations (6.1). These equations are indicated by black arrows in Figure 6.1. The superfluous grid points marked red in the figure at the vertices of the interface (and more grid

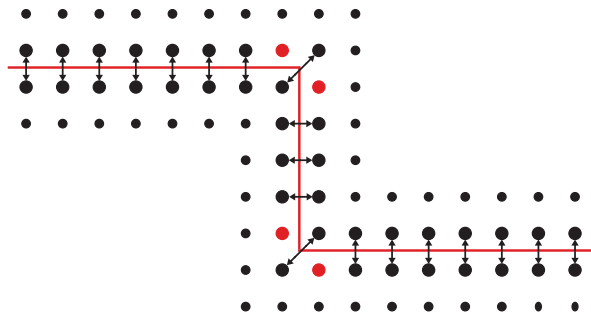


FIG. 6.1. Location of the grid points at the interface. The red points are additional points whose treatment is explained in Figure 6.2. The arrows indicate how two values $V(0+)$ and $V(0-)$ are connected by equations (6.1).

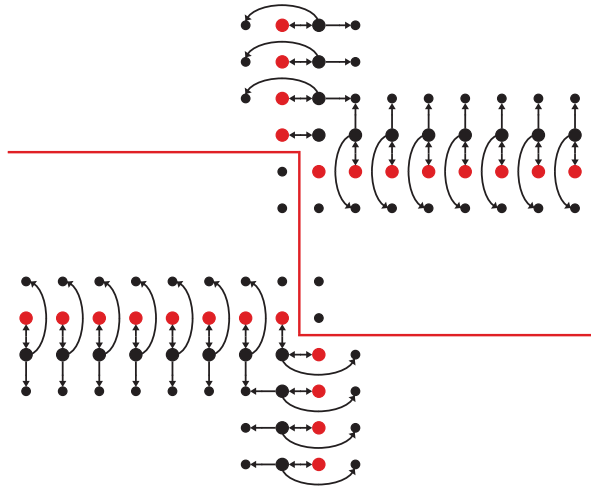


FIG. 6.2. The superfluous red grid points are located in rows and columns that start at the vertices of the interface. These superfluous points are identified with neighboring black points as indicated by the arrows between a red and a black point each. The other arrows between two black points show which grid points are linked in the finite-volume discretization of the Laplace operator.

points in rows and columns starting there indicated in Figure 6.2) are identified with neighboring points by trivial equations.

Furthermore, the black points at the vertices of the interface require special attention due to their location. The equations

$$V_{i,j,k} - V_{i-1,j-1,k} = \alpha,$$

$$A(0+) \frac{V_{i+1,j+1,k} - V_{i,j,k}}{\sqrt{\Delta x^2 + \Delta y^2}} - A(0-) \frac{V_{i-1,j-1,k} - V_{i-2,j-2,k}}{\sqrt{\Delta x^2 + \Delta y^2}} = \gamma$$

for these points are similar to the equations (6.1).

As mentioned above, the superfluous red grid points are identified with their neighbors and the correct side so that the finite-volume discretization of the Poisson equation ignores these points (see Figure 6.2). This can also be viewed as a shift in

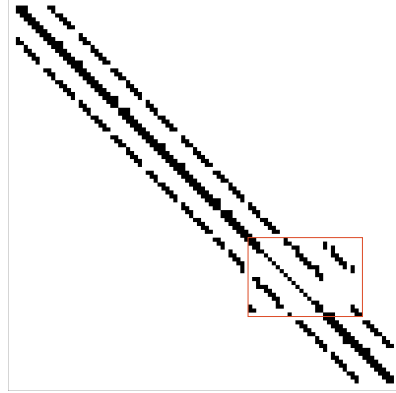


FIG. 6.3. *The system matrix. The red box indicates the points associated with the vertical part of the interface.*

space of the points used for computation. Hence, the discretization of the x -derivative in the finite-volume discretization reads

$$-\left(A_{i+\frac{1}{2},j} \frac{V_{i+1,j,k} - V_{i,j,k}}{\Delta x} - A_{i-\frac{3}{2},j} \frac{V_{i,j,k} - V_{i-2,j,k}}{\Delta x}\right) \Delta y \Delta z, \quad (6.2)$$

and the y - and z -derivatives give rise to analogous terms.

In summary, this complicated numbering scheme with additional grid points that are identified later implies that the band structure of the finite-volume discretization of the Laplace operator is retained, i.e., it exhibits almost the same band structure. An example is shown in Figure 6.3. The difference (marked by a red box) from the usual band structure comes from the numbering scheme at the vertical part of the interface which moves the band structure outwards. The missing points in the band structure are due to the identification of superfluous points with neighbors and result in a simpler system of linear equations.

This implementation of the interface conditions is optimal in the sense that there is no computational penalty that must be paid for using the interface conditions (and the homogenized equation), since the computational effort is determined by the bandwidth.

7. Numerical results

In order to compare the numerical simulation results obtained from the system of equations (2.4) with measurements, a real-world experimental structure is considered [2,3,11]. It consists of a silicon nanowire with a silicon-dioxide layer placed on a silicon substrate immersed in an aqueous solution (see Figure 1.1). The interface conditions are located between the silicon-dioxide layer and the aqueous solution and they model the biofunctionalized boundary layer of the sensor. The boundary conditions are the Dirichlet conditions for the ohmic contacts at the source and drain ends of the nanowire, for the back-gate at V_b below the substrate, and for the electrode at V_e in the liquid. Zero Neumann boundary conditions are used everywhere else.

For the comparison with experimental data from [26], we simulated a 500nm long biosensor with a 120nm wide and 40nm high silicon nanowire. The nanowire is n-doped with a doping concentration of 10^{17}cm^{-3} and a back-gate voltage of $V_b =$

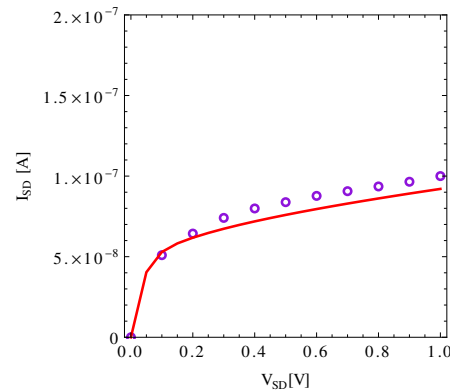


FIG. 7.1. A simulated current-voltage characteristic (dotted line) and an experimental characteristic (solid line) with a back-gate voltage of 5V. The source-drain voltage varies between 0V and 1V.

5V is used. The results are shown in Figure 7.1. The simulated current-voltage characteristics and the experimental data are in very good agreement, which shows the ability of the three-dimensional PDE model in (2.4) to reproduce the physics of this kind of sensor. Note that also the slopes at $V_{SD} = 0$, i.e., the transconductances, agree.

A key problem in this field is the determination of several physical parameters that cannot be determined experimentally. Hence a more detailed study based on the present model can be found in [27] in order to aid the rational design and optimization of these sensors by simulation.

8. Conclusions

Proofs of existence and local uniqueness for a 3d nonlinear system of PDEs with interface conditions were presented. The PDE system serves as a model for the self-consistent simulation of field-effect sensors such as bio- and gas sensors. The model contains two interface conditions for the electric potential and the electric displacement and is based on the drift-diffusion equations and the Poisson-Boltzmann equation. The main results of existence and local uniqueness around thermal equilibrium hold true under reasonable assumptions also on the microscopic model for the boundary layer that yields the values of the interface conditions. The key methods for these results are the Leray-Schauder fixed-point theorem, a maximum principle for nonlinear PDEs, and the implicit-function theorem.

Furthermore, this model shows very good quantitative agreement with experimental data. Importantly, the simulations are 3d and self-consistent, i.e., the macroscopic dipole-moment density and the macroscopic surface-charge density are updated in every iteration in dependence on the potential. Consequently we believe that this PDE model will prove to be useful for the rational design of field-effect sensors.

9. Acknowledgment. The authors acknowledge discussions with Alena Buljha, Peter Markowich, Christian Schmeiser, and Martin Vasicek.

This work was supported by the FWF (Austrian Science Fund) project No. P20871-N13 and by the WWTF (Viennese Science and Technology Fund) project No. MA09-028. This publication is based on work supported by Award No. KUK-I1-007-43, funded by the King Abdullah University of Science and Technology (KAUST).

REFERENCES

- [1] G. Zheng, F. Patolsky, Y. Cui, W.U. Wang, and C.M. Lieber, *Multiplexed electrical detection of cancer markers with nanowire sensor arrays*, Nature Biotech., 23, 1294–1301, 2005.
- [2] E. Stern, J.F. Klemic, D.A. Routenberg, P.N. Wyrembak, D.B. Turner-Evans, A.D. Hamilton, D.A. LaVan, T.M. Fahmy, and M.A. Reed, *Label-free immunodetection with CMOS-compatible semiconducting nanowires*, Nature, 445, 519–522, 2007.
- [3] E. Stern, A. Vacic, N.K. Rajan, J.M. Criscione, J. Park, B.R. Ilic, D.J. Mooney, M.A. Reed, and T.M. Fahmy, *Label-free biomarker detection from whole blood*, Nature Nanotech., 5, 138–142, 2010.
- [4] B. Tian, T. Cohen-Karni, Q. Qing, X. Duan, P. Xie, and C.M. Lieber, *Three-dimensional, flexible nanoscale field-effect transistors as localized bioprobes*, Science, 329, 830–834, 2010.
- [5] S. Sorgenfrei, C.-Y. Chiu, R.L. Gonzalez, Jr., Y.J. Yu, P. Kim, C. Nuckolls, and K.L. Shepard, *Label-free single-molecule detection of DNA-hybridization kinetics with a carbon nanotube field-effect transistor*, Nature Nanotech., 6, 126–132, 2011.
- [6] A. Tischner, T. Maier, C. Stepper, and A. Köck, *Ultrathin SnO₂ gas sensors fabricated by spray pyrolysis for the detection of humidity and carbon monoxide*, Sens. Actuators B: Chem., 134, 796–802, 2008.
- [7] A. Köck, A. Tischner, T. Maier, M. Kast, C. Edtmaier, C. Gspan, and G. Kothleitner, *Atmospheric pressure fabrication of SnO₂-nanowires for highly sensitive CO and CH₄ detection*, Sens. Actuators B: Chem., 138, 160–167, 2009.
- [8] H. Huang, C.Y. Ong, J. Guo, T. White, M.S. Tsea, and O.K. Tana, *Pt surface modification of SnO₂ nanorod arrays for CO and H₂ sensors*, Nanoscale, 2, 1203–1207, 2010.
- [9] C. Ringhofer and C. Heitzinger, *Multi-scale modeling and simulation of field-effect biosensors*, ECS Transactions, 14(1), 11–19, 2008.
- [10] C. Heitzinger, N.J. Mauser, and C. Ringhofer, *Multiscale modeling of planar and nanowire field-effect biosensors*, SIAM J. Appl. Math., 70(5), 1634–1654, 2010.
- [11] N. Elfström, R. Juhasz, I. Sychugov, T. Engfeldt, A. E. Karlström, and J. Linnros, *Surface charge sensitivity of silicon nanowires: Size dependence*, Nano Lett., 7(9), 2608–2612, 2007.
- [12] A.G. Cherstvy, *Electrostatic interactions in biological DNA-related systems*, Phys. Chem. Chem. Phys., 13, 9942–9968, 2011.
- [13] A. Fort, S. Rocchi, M.B. Serrano-Santos, R. Spinicci, and V. Vignoli, *Surface state model for conductance responses during thermal-modulation of SnO₂-based thick film sensors: Part I—model derivation*, IEEE Transactions on Instrumentation and Measurement, 55(6), 2102–2106, 2006.
- [14] A. Bulyha and C. Heitzinger, *An algorithm for three-dimensional Monte-Carlo simulation of charge distribution at biofunctionalized surfaces*, Nanoscale, 3(4), 1608–1617, 2011.
- [15] P.A. Markowich, *The Stationary Semiconductor Device Equations*, Springer-Verlag, Vienna, 1986.
- [16] P.A. Markowich, C.A. Ringhofer, and C. Schmeiser, *Semiconductor Equations*, Springer-Verlag, Vienna, 1990.
- [17] N. El Ghani and N. Masmoudi, *Diffusion limit of the Vlasov-Poisson-Fokker-Planck system*, Commun. Math. Sci., 8(2), 463–479, 2010.
- [18] C. Buet and St. Dellacherie, *On the Chang and Cooper scheme applied to a linear Fokker-Planck equation*, Commun. Math. Sci., 8(4), 1079–1090, 2010.
- [19] C. Heitzinger, Y. Liu, N.J. Mauser, C. Ringhofer, and R.W. Dutton, *Calculation of fluctuations in boundary layers of nanowire field-effect biosensors*, J. Comput. Theor. Nanosci., 7(12), 2574–2580, 2010.
- [20] N. Ben Abdallah, P. Degond, P. Markowich, and C. Schmeiser, *High field approximations of the spherical harmonics expansion model for semiconductors*, Z. Angew. Math. Phys., 52(2), 201–230, 2001.
- [21] N. Ben Abdallah, F. Méhats, and N. Vauchelet, *Diffusive transport of partially quantized particles: Existence, uniqueness and long-time behaviour*, Proc. Edinburgh Math. Soc., (2), 49(3), 513–549, 2006.
- [22] C. Heitzinger and C. Ringhofer, *A transport equation for confined structures derived from the Boltzmann equation*, Commun. Math. Sci., 9(3), 829–857, 2011.
- [23] Z. Ding, *A proof of the trace theorem of Sobolev spaces on Lipschitz domains*, Proc. Amer. Math. Soc., 124(2), 591–600, 1996.
- [24] L.A. Caffarelli and X. Cabré, *Fully Nonlinear Elliptic Equations*, Oxford University Press, 1995.
- [25] J.W. Jerome, *Consistency of semiconductor modeling: An existence/stability analysis for the*

- stationary Van Roosbroeck system*, SIAM J. Appl. Math., 45, 565–590, 1985.
- [26] N. Elfström, A.E. Karlström, and J. Linnros, *Silicon nanoribbons for electrical detection of biomolecules*, Nano Lett., 8(3), 945–949, 2008.
- [27] S. Baumgartner, M. Vasicek, A. Bulyha, and C. Heitzinger, *Optimization of nanowire DNA sensor sensitivity using self-consistent simulation*, Nanotech., 22(42), 425503/1–8, 2011.